

## Disclaimer

This note has not been internally reviewed by the DØ Collaboration. Results or plots contained in this note were only intended for internal documentation by the authors of the note and they are not approved as scientific results by either the authors or the DØ Collaboration. All approved scientific results of the DØ Collaboration have been published as internally reviewed Conference Notes or in peer reviewed journals.

D0 Note 1107  
February 1991

**THE EXPERIMENTAL SETUP FOR STUDYING  
THE CHARACTERISTICS OF THE MODULES  
OF THE LIQUID ARGON CALORIMETER  
FOR THE D0 DETECTOR  
(REVIEW)**

*S. Cherny*

*Institute for High Energy Physics, Protvino, USSR*

The activities on the D0 detector under development at Fermilab [1,2] for colliding beam studies are aimed at versatile goals. One of them is to carry out beam studies of the characteristics of single modules of the liquid argon calorimeter. To achieve this goal a special area, NWA, in the neutrino beam line direction was allocated in the experimental area of the Fermilab. In addition, a test cryostat to be placed in the liquid argon medium of the modules to be tested has been designed and manufactured, the data readout system assembled, secondary beams for tests formed and the beam diagnostics system installed. Some of the versatile goals of these activities are as follows [3]:

- study of the effects of anomalous currents;
- choice of the working point from the high-voltage module supply;
- study of the module mapping;
- measurement of the signal linearity;
- measurement of the electron/pion response in the particle momentum range;
- charting the detector response versus the pseudorapidity ( $\eta$ ) and angle ( $\varphi$ ) values;
- study of the detector response close to the boundaries of the uranium plates, spacers and module edges;
- study of pedestals and their long-term stability;
- and also obtaining a number of other characteristics required for on- and off-line data handling with the liquid argon calorimeter as a component of the detector D0.

## GENERAL LAYOUT OF THE SETUP

Figure 1 shows the general layout of the experimental setup in the NWA area. The test cryostat with the modules of liquid argon calorimeter to be tested inside is installed in a separate protected area. Deepening the floor by 10' allows one to install an efficient system of the cryostat displacements for various spatial scannings with respect to the secondary beam position. The entrances to the area have a system interlocking beam extraction with the door open for personnel radiation safety considerations. Behind the cryostat downstream there is a demountable wall made of 3' concrete blocks which protects the personnel against the beam. Farther behind the wall there is a "clean room" for assembling the calorimeter modules. The Ar and  $N_2$  dewar for the cryogenic system of the cryostat are beyond the NWA out-of-doors. The test area is also equipped with electronics decks, the secondary beam diagnostics system and electronics for processing the signals from the modules. The set of the preamplifiers of the signals coming from the modules, are fixed directly to the cryostat. There are several rooms adjacent to the NWA building. The control room for the cryogenic system, electronics crates data acquisition and interface with the computer, high-voltage power supplies for the modules and beam detectors are located in one of these rooms. Other control rooms are assigned for beam line control, the computer stations for signal processing and control of the NWA complex.

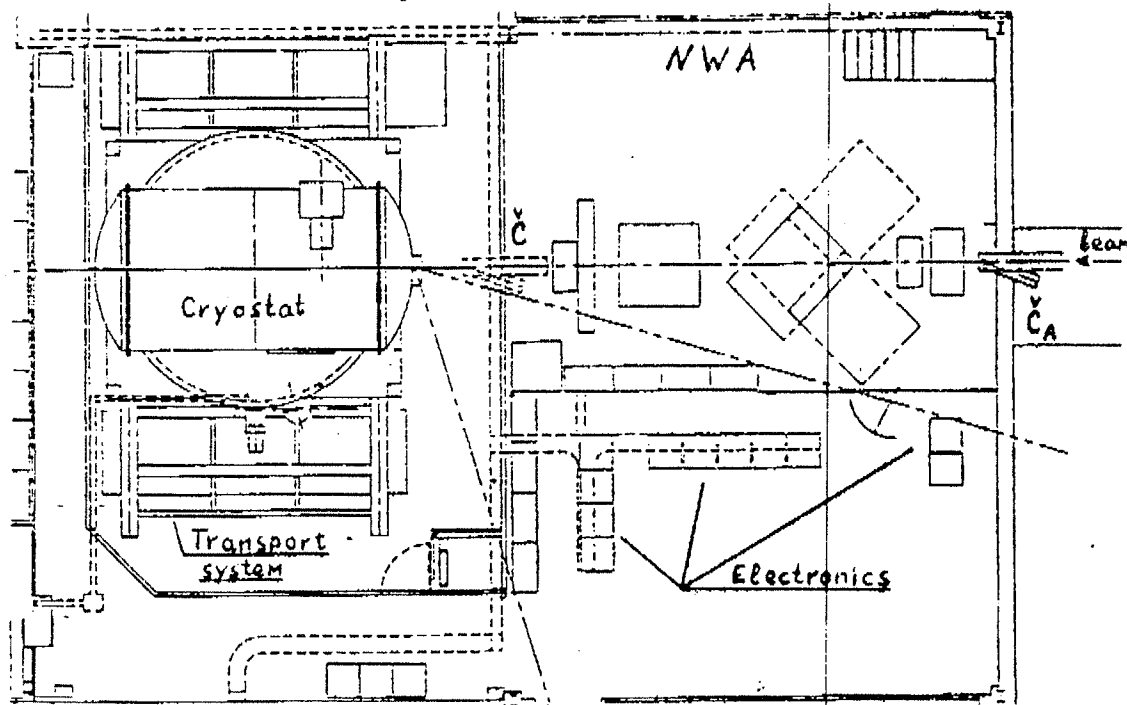


Fig.1. Equipment layout in the NWA area.

## THE SYSTEM OF CRYOSTAT DISPLACEMENTS

The cryostat transport system allowing one to explore various sections of the test cryostat with the particle beam ensures the following displacements:

- $190^{\circ}$  rotation around the vertical cryostat axis ( $\theta$ );
- $\pm 15^{\circ}$  rotation around the horizontal cryostat axis ( $\varphi$ );
- 144" horizontal motion (X);
- 30" vertical motion (Y).

The large range of the cryostat vertical rotations ( $\pm 5^{\circ}$  from the beam axis plus  $180^{\circ}$ ) was determined by the peculiarities of the assembling procedure for the modules in the cryostat though physical measurements require a smaller rotation range,  $-5^{\circ} < \theta < +40^{\circ}$ . According to the procedure mentioned above the modules will be assembled in the clean room, then the first modules will be placed downstream, the cryostat will be rotated by  $180^{\circ}$  and the next modules will be placed from the free end of the cryostat. Figure 2 shows the general layout of the displacement system with the cryostat assembled in it.

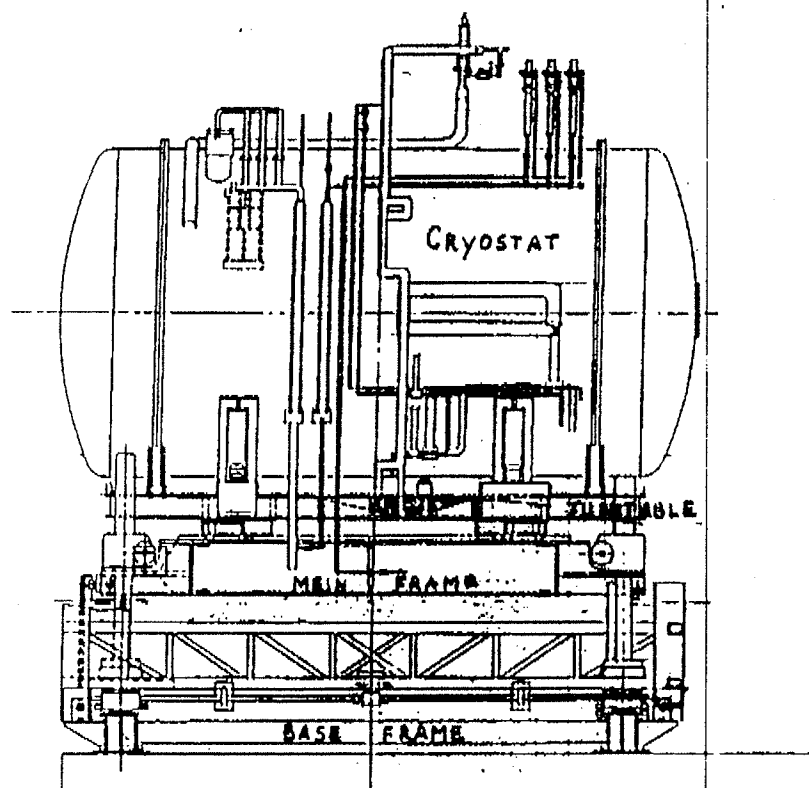


Fig.2. Test cryostat with the transport system.

## THE CRYOSTAT

The cryostat [4] consists of inner and outer stainless steel vessels. The inner vessel is 9' and the outer one is 9'-8" in diameter and about 20' long. The fiducial volume of the cryostat without modules is 7.800 gallons. The argon is cooled with two nitrogen condensers located at the top inside the cryostat. The inner and outer vessels are separated by the intervessel gap filled with superinsulation with subsequent vacuum pumping. The cable connectors of the modules are brought out through two cable ports. The cryostat has some inherent design features. The sections of the inner cylinder and cover to be welded have no flanges. The calorimeter modules are protected against direct ingress of dirt during welding by the horseshoe unit. The cable ports of the outer vessel are sealed with the help of indium-alloy O-ring. The vacuum seals of the outer vessel are made from rubber sealing compound.

Figure 3 shows the layout of the modules inside the test cryostat for testing the modules of the end calorimeter of the D0 detector, as for their location in the end-cup calorimeter D0 see fig.4. In front of the electromagnetic module there is a plastic excluder designed to decrease the mass of the matter along the beam path up to the modules. The ratio of the plastic excluder specific mass to that of the liquid argon is 1/100. The 1.7" thick aluminium and 10" thick steel plates (see fig.3) are used to simulate the material of the walls of the end calorimeter.

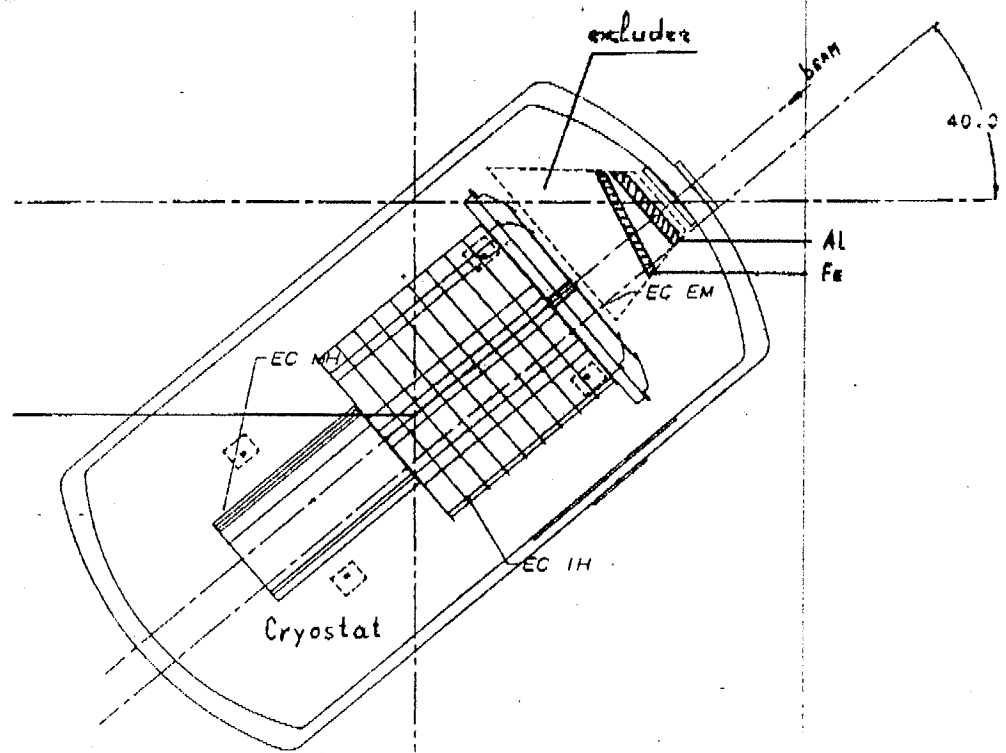


Fig.3. Location of end cap calorimeter modules D0 inside the test cryostat.

To place the modules inside the cryostat a special device is used, which provides an air cushion for the motion of the girder and modules on it along the mounting table. The contact surfaces of the support and table are covered with a thin layer of teflon in order to reduce friction caused by variation in the linear dimensions during cool down. In addition, this coating hinders such an effect as metal-metal diffusion and the setting of the support and table materials. Since the table support system is a source of a large heat influx the supporting pillars are equipped with additional heat exchangers cooled by liquid nitrogen.

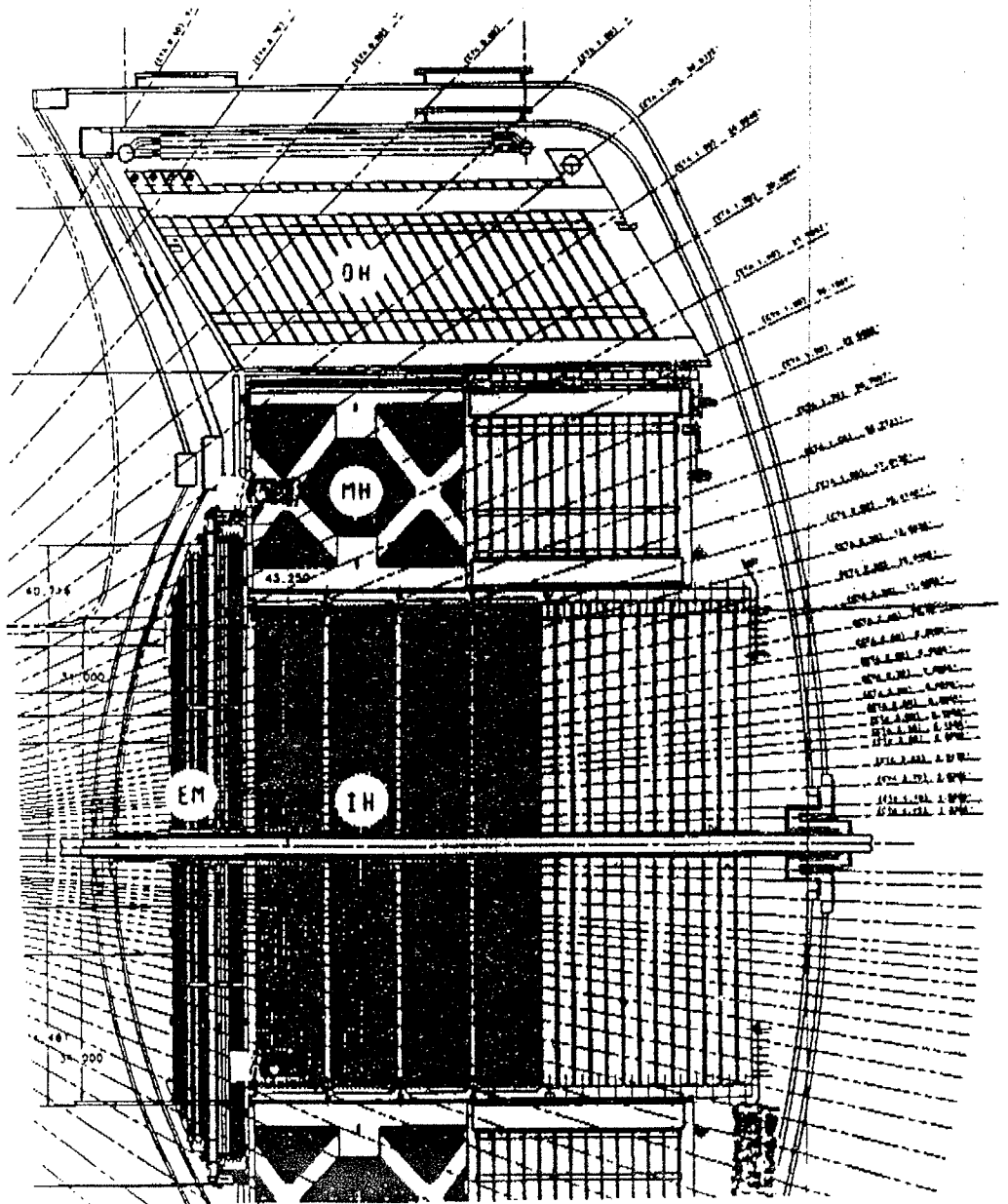


Fig.4. End cap calorimeter of the detector D0.

## THE CRYOGENIC SYSTEM

The cryogenic system supplies the test cryostat with ultra high purity liquid argon. The layout of the cryogenic supply is shown in fig.5. Eleven parameters measured automatically, are monitored and maintained at the specified level with the help of the control system of the cryogenic complex. The measured parameters include the following ones: gaseous argon pressure and liquid argon temperature, the pressure of gas and temperature in the argon purity meter placed on the transfer line, nitrogen level and pressure in the dewar, nitrogen pressure and temperature in the condensers. The cryogenic system maintains the basic parameters within the following ranges:

- temperature  $\pm 1^{\circ}$ ;
- pressure  $\pm 5$  PSIA;
- argon purity  $< 1.2 \times 10^{-6} O_2/Ar$ .

The above parameters are the technological cryogenic parameters. Besides, there is a set of cryogenic data incorporated in the common physical data base, which is not monitored in the cryogenic control room. These include ~70 points of temperature measured on the cryostat and calorimeter modules, 2 pressure points in the cryostat and 5 points of argon purity measurements [5]. These data are used to analyze the situation during cool down.

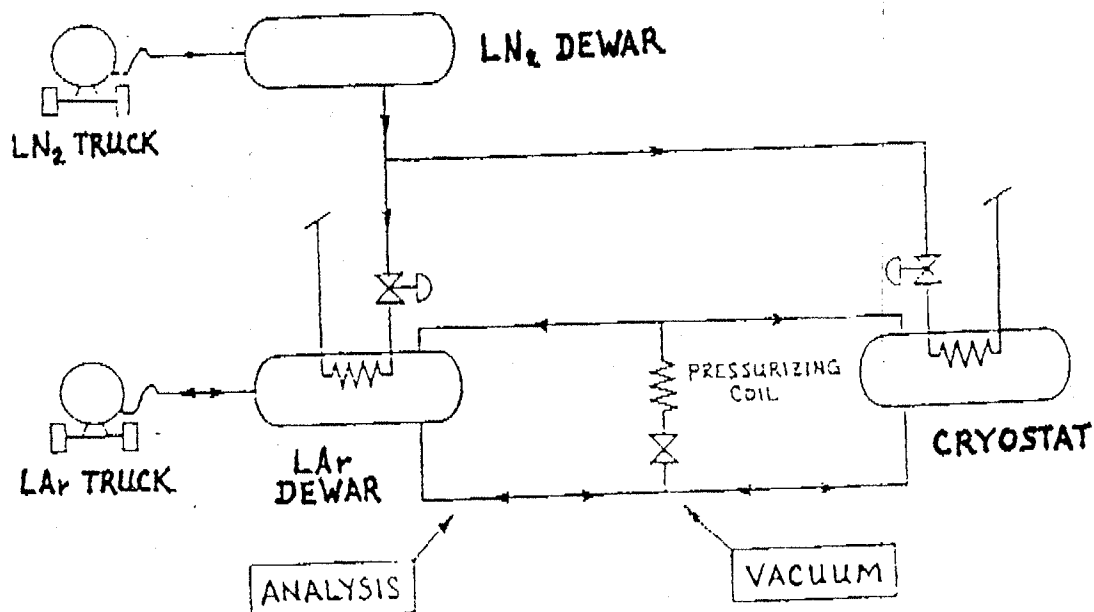


Fig.5. Cryogenic system of the test cryostat.

## THE HIGH-VOLTAGE POWER SUPPLY SYSTEM FOR THE CALORIMETER MODULES

Figure 6 presents the layout of the high-voltage power supply system [6]. Eighteen high-voltage power supply sources energize the calorimeter modules, grouped into 18 sets. The instability level of the supply voltage is  $\sim 1\%$ , and the noise is 3 nA. The high-voltage level (to 3kV) is set and measured manually, whereas the current of the power supplies are measured automatically and their variations can be traced during a long period run.

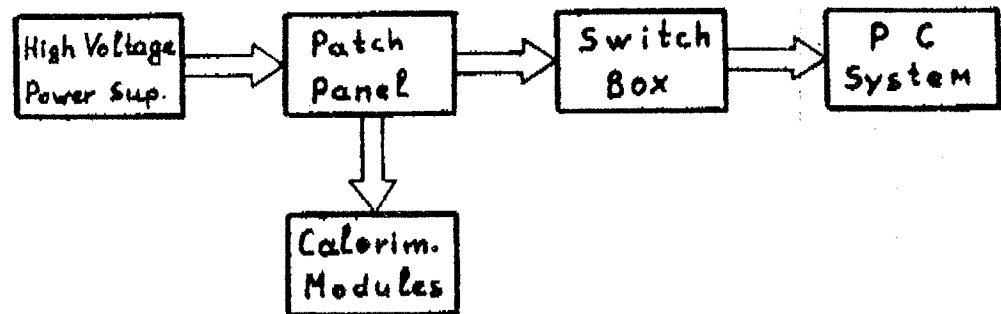


Fig.6. Block-diagram of HV power supply for the calorimeter modules.

## THE ELECTRONICS OF THE TEST CRYOSTAT

The electric signals coming from the calorimeter modules enter the preamplifiers [7] placed next to the cable port of the cryostat. The input preamplifier impedance is 15-20 Ohm, providing a signal rise time at the preamplifier output not larger than 100 nsec. The main problem, one faces when developing a preamplifier for the liquid argon calorimeter, is to ensure a good signal-to-noise ratio together with a fast response [8]. After studying the noise characteristics of some transistors the JFET type was chosen as more preferable [9]. One of several noise sources during amplification of a signal coming from the elementary cell (see fig.7) was supposed to be a uranium plate. As for its electron surface emission into the working gap it was supposed to be intercepted by the counteraction of the electric field, when a high voltage of the negative polarity was applied to the electrode coated by a resistive layer. However, as the major source of electronic noise turned out to be the resistive coat, the polarity of the high voltage applied was reversed and the preamplifier circuit was modified for the complementary transistors (see fig.8). After these modifications the noise level was reduced down to the tolerable one and presently the noise components from the calorimeter cell and the preamplifier are about equal.



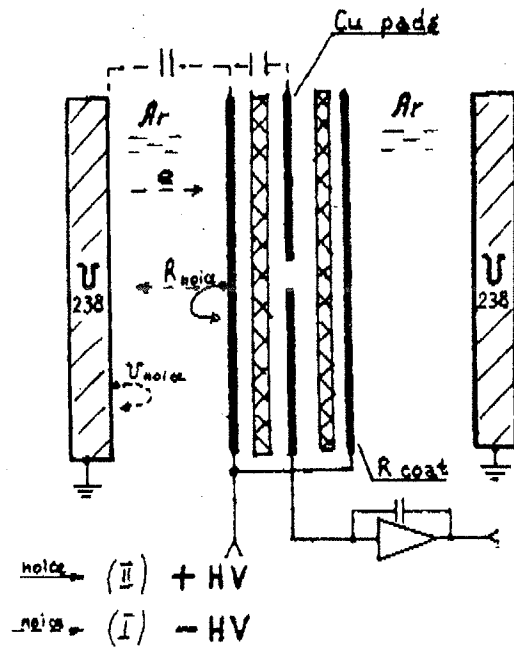


Fig.7. Scheme of the calorimeter modules cell.

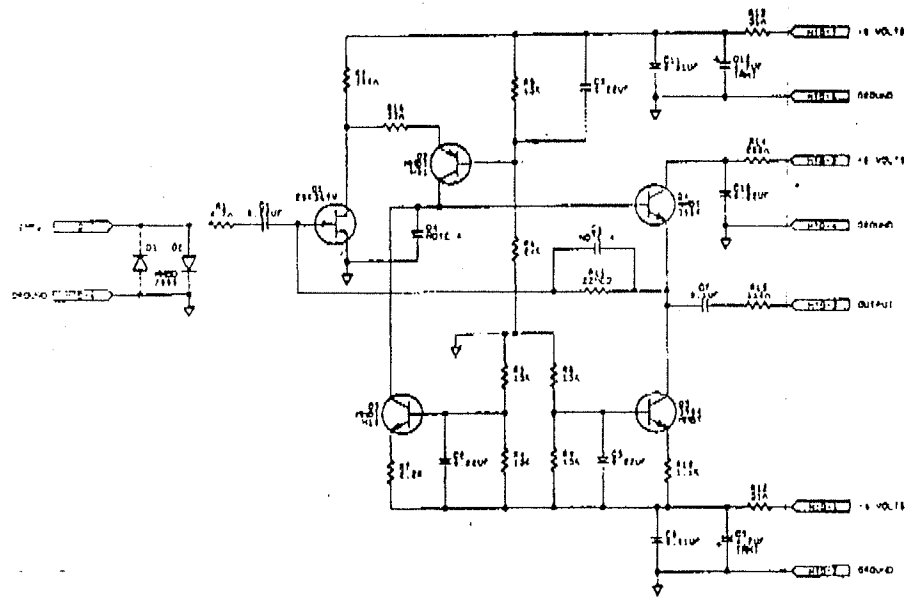


Fig.8. Electrical circuit of the charge preamplifier.

The signal from the preamplifier goes into the base line subtraction (BLS) [10] whose function is to gate the signal from the trigger signals and subtract the pedestals. The BLS module includes 48 processing channels for the central calorimeter (44 channels for the end calorimeter). The analog processing channel consists of the circuit measuring the base signal before the peak, signal of peak, subtracting the signals (see fig.9) and the buffer cascade which holds the difference (see fig.10). The same block contains the circuits for the power supply sources, those for the module temperature control, for trigger and testing the module. The analog-to-digital convertor (ADC) receiving the signal from the BLS has a range of  $2^{15}$  counts and nonlinearity of  $< 0.05\%$ . The ADC sensitivity is  $100 \mu\text{V}/\text{counts}$  and the typical output pedestal level is 250 counts. The ADC signal is fed into the computer to be further processed.

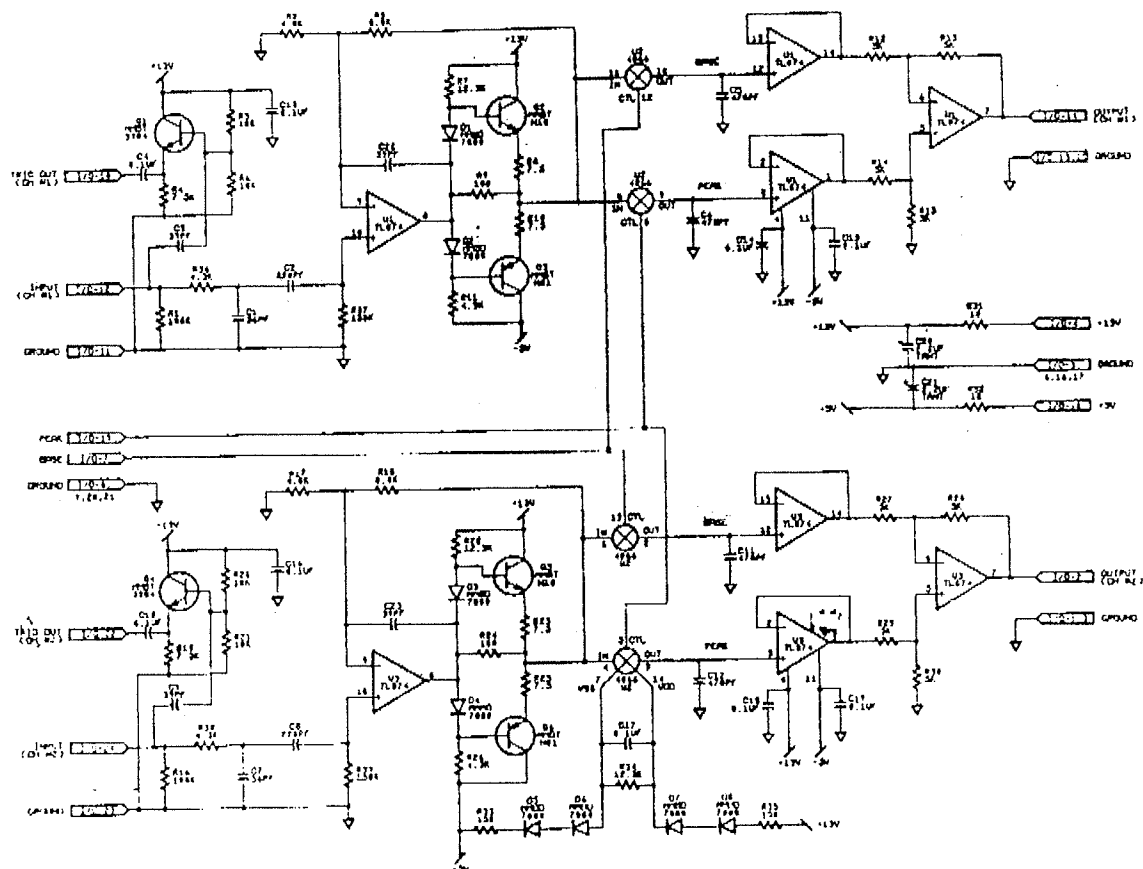


Fig.9. Electrical circuit of the dual base-peak sample/hold.

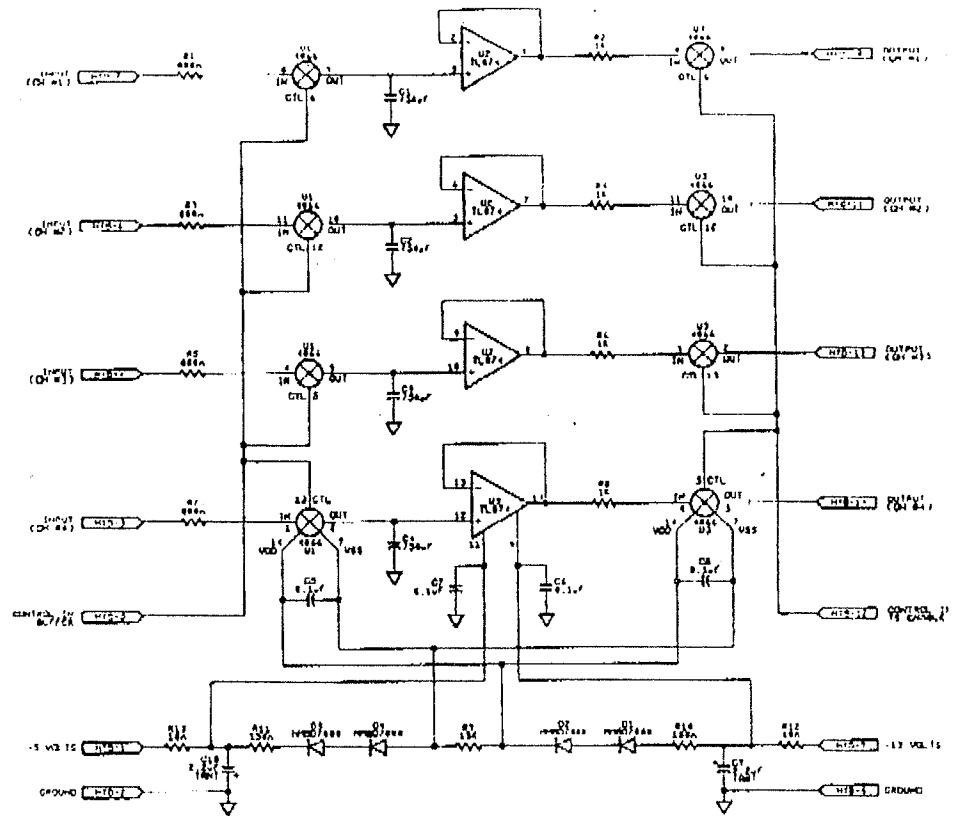


Fig.10. Electrical circuit of the quad buffer/time slice enable.

## SECONDARY BEAM FOR THE TEST CRYOSTAT

The beam line of secondary particles forms the beams for methodical studies in the NWA area in the (10-150) GeV/c momentum range. The layout of the beam line equipment is shown in fig.11. The 800 GeV protons extracted from the machine are transferred onto the  $6 \times 6 \times 12''$  Al target placed in the NW3 area. According to the routine operational beam line mode, particle extraction lasts about 20 sec while the total machine cycle is about 70-sec. The secondary beams are formed by the magnetic and optic beam line system [11](see fig.12) and transported into the NWA test area. The optical scheme envisages beam shaping in three modes, whose specific features are determined by their applications in the study of the properties of the modules for the calorimeter detectors [12]. An important parameter of the modules is response of the detector to a hadron and electron passing through it.

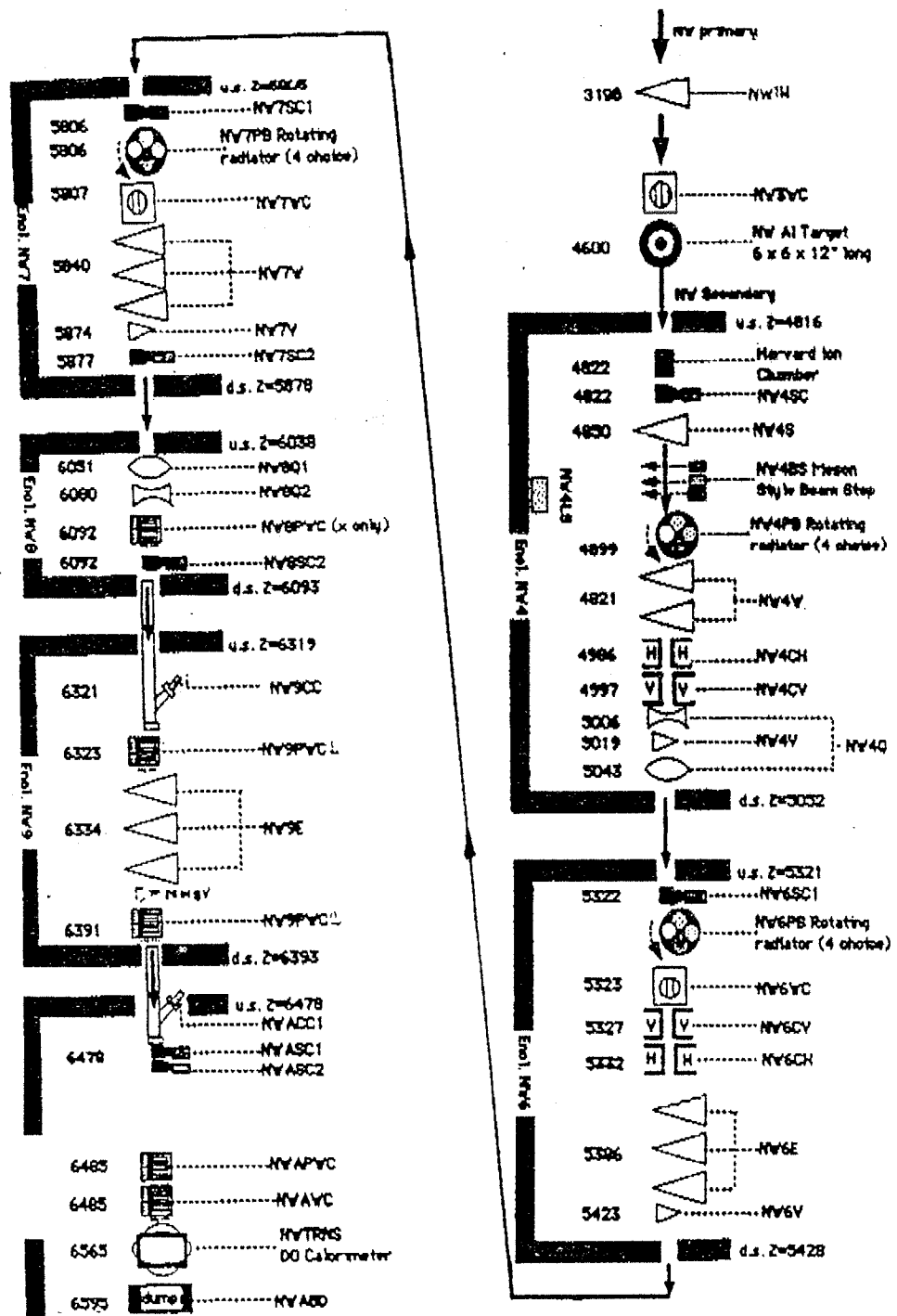


Fig.11. Schematic layout of the NW beam line equipment.

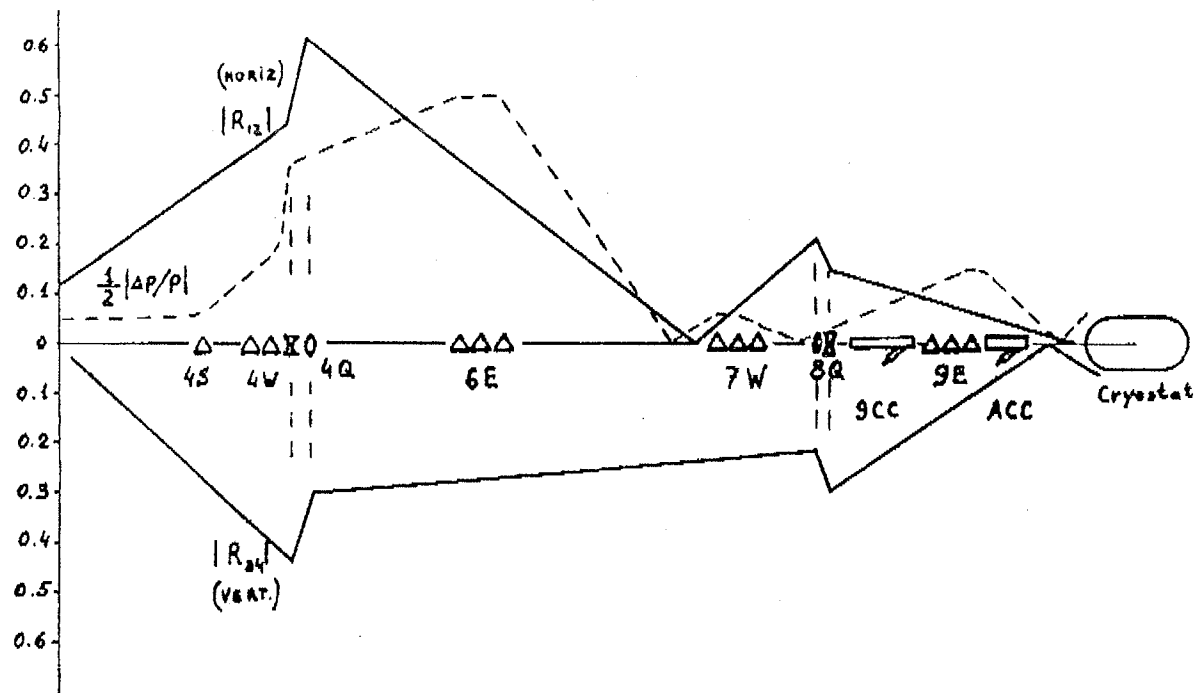


Fig.12. Optical scheme of forming secondary particle beam of the NW beam line.

Therefore the main two operational beam line modes are the shaping of purified pion and electron beams. The third mode is the shaping of the beam having a natural particle mixture. In the first case, the beam is purified from electrons with 1/4" thick lead plates placed in the NW6 and NW7 areas (see fig.11), which suppress the electrons below the level of  $10^{-4}$ . To achieve the pure electron beam mode, the purifying magnet NW4S is turned on, that deflects the charged particles from the beam line path. In this, the  $\pi^0$ -mesons produced on the target, when decaying, produce  $\gamma$ -quanta which, in their turn, interact with the convertor matter to produce an  $e^+e^-$ -pair. Typically  $2 \times 10^{11}$  protons are spilled onto the target, in which case the particle fluxes in the beam line can be estimated from the curve in fig.13.

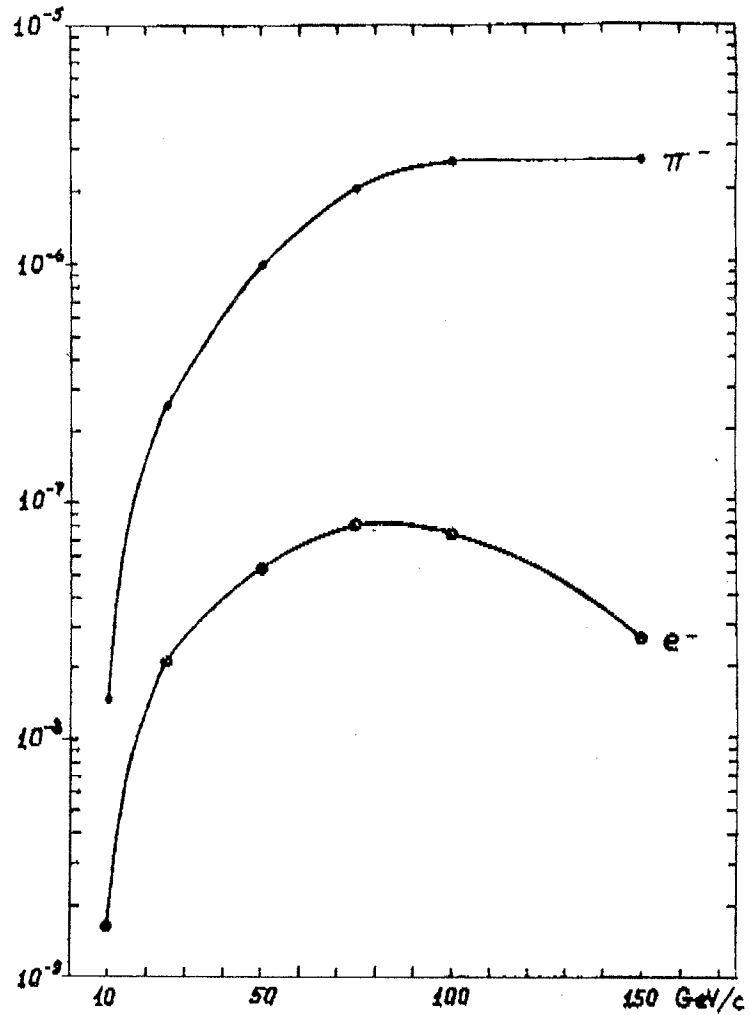


Fig.13. Pion and electron rates per 800 GeV/c proton.

## THE BEAM DIAGNOSTICS DEVICES

Proportional wire chambers [13] are used to detect the beam profiles in the beam line. Their design is such that with an effective wire-to-wire distance of about 0.5 mm they can measure the beam profiles. To measure the beam content, a system of two gas threshold Cherenkov counters [14] is used, that includes a scintillation telescope made for three scintillation plates resolving in the beam line aperture the region having an area of about  $4 \times 4''$ . The first Cherenkov detector (NW9CC) about 230' long is placed between the NW8 and NW9 areas, while the second one (NWACC) 98' long is placed in the spacing between the NW9 and NWA areas.

Helium, used as a radiator in the Cherenkov counter, fills the 12" pipe and its working pressure range is 2 psia-14.7 psia. Photomultipliers of the RSA-C31000M operating from an anode voltage of about 2400 V register Cherenkov radiation.

The design values of the threshold pressures for these counters are given in fig.14. The routine operational mode of these detectors is the measurement of the coincidence of the signals from two Cherenkov counters with those from the telescope made of three scintillation counters. Figures 15 and 16 show the curves illustrating the efficiency of recording particles of various momenta [15].

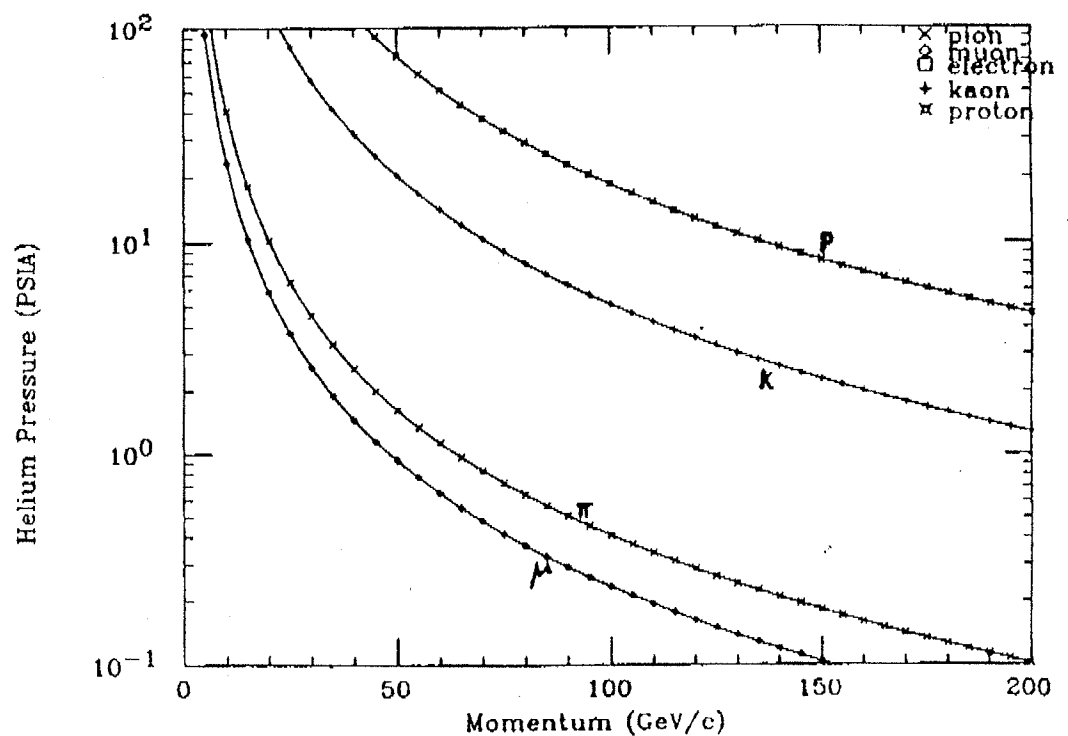


Fig.14. Threshold pressure of Cherenkov counter versus particle momentum.

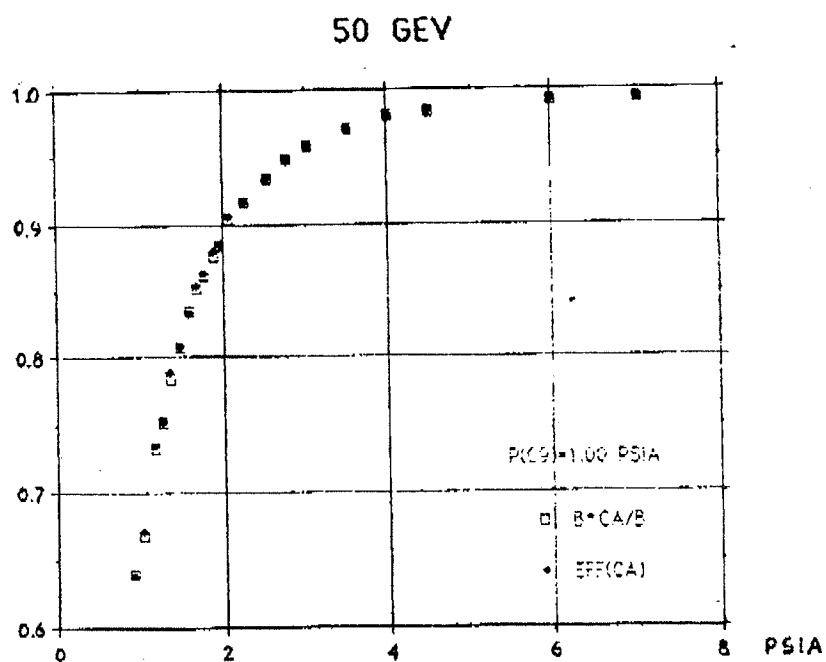


Fig.15. Cherenkov counter efficiency versus He pressure for electron beam.

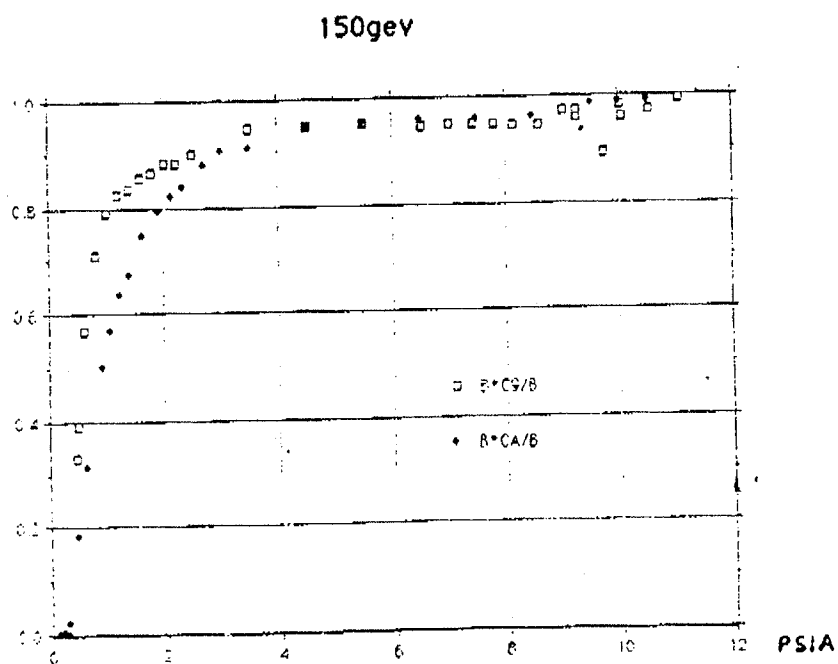


Fig.16. Cherenkov counter efficiency versus He pressure for pion beam.



## CONCLUSIONS

The scheme of the devices described in the present note allows the calibration of single D0 detector elements in the beam line from 10 upto 150 GeV/c. The beam parameters vary easily in a wide range, thus allowing one to carry out different measurements. To conclude, the author would like to express his sincere gratitude to P.Bhat, P.Draper, S.Durston, H.Haggerty, B.Karsh, G.Krafczyk, R.Lipton, D.Owen, T.Spadafora, M.Tartaglia for helpful discussions and comments.

## REFERENCES

1. D0 Design Report, Fermilab (1984).
2. P.Grannis, D0 Note 558, May (1987).
3. Calorimeter Test Beam Meeting, Apr. (1990).
4. Engineering Note SD-37B, Test Beam Cryostat, May (1990).
5. G.Blazey, D0 Note 699, May (1988); G.Blazey, D0 Note 940, March (1990).
6. S.Durston, Private Communications, May (1990).
7. V.Radeka, IEEE Trans. Nucl. Sci. NS-21 (1974), p. 51.
8. V.Radeka and S.Rescia, NIM, A265 (1988), p. 228.
9. V.Radeka, NIM, 226 (1984), p. 209.
10. Calorimeter electronics review, D0 note 609, Aug. (1987), see also F.Borcherding, D0 note 945, Apr. (1990).
11. P.Bhat, Private communications, May (1990).
12. H.Piekarz, D0 note 932, Febr. (1990).
13. H.Fenker, FNAL TM-1179, Febr. (1983).
14. P.Draper, Private communications, Aug. (1989).
15. M.Tartaglia, Private communications, May (1990).